Surface tension, viscosity, and rheology of water-based nanofluids: a microscopic interpretation on the molecular level

3 **AUTHORS**, INCLUDING:

Yuan-Yuan Duan

Tsinghua University

110 PUBLICATIONS   **999** CITATIONS

Surface tension, viscosity, and rheology of water-based nanofluids: a microscopic interpretation on the molecular level

Gui Lu · Yuan-Yuan Duan · Xiao-Dong Wang

Abstract Nanofluids are suspensions of nanometer-sized particles which significantly modify the properties of the base fluids. Nanofluids exhibit attractive properties, such as high thermal conductivity, tunable surface tension, viscosity, and rheology. Various attempts have been made to understand the mechanisms for these property modifications caused by adding nanoparticles; however, due to the lack of direct nanoscale evidence, these explanations are still controversial. This work calculated the surface tension, viscosity, and rheology of gold–water nanofluids using molecular dynamics simulations which provide a microscopic interpretation for the modified properties on the molecular level. The gold–water interaction potential parameters were changed to mimic various nanoparticle types. The results show that the nanoparticle wettability is responsible for the modified surface tension. Hydrophobic nanoparticles always tend to stay on the free surface so they behave like a surfactant to reduce the surface tension. Hydrophilic nanoparticles immersed into the bulk fluid impose strong attractive forces on the water molecules at the free surface which reduces the free surface thickness and increases the surface tension of the nanofluid. Solid-like absorbed water layers were observed around the nanoparticles which increase the equivalent nanoparticle radius and reduce the mobility of the nanoparticles within the base fluid which increases the nanofluid viscosity. The results show the water molecule solidification between two or many nanoparticles at high nanoparticle loadings, but the solidification effect is suppressed for shear rates greater than a critical shear rate; thus Newtonian nanofluids can present shear-thinning non-Newtonian behavior.

Keywords Surface tension · Viscosity · Rheology · Molecular level · Nanofluid · Colloids

G. Lu · Y.-Y. Duan (✉)
Key Laboratory for Thermal Science and Power Engineering of MOE, Tsinghua University, Beijing 100084, People's Republic of China
e-mail: yyduan@mail.tsinghua.edu.cn;
yyduan@tsinghua.edu.cn

G. Lu
Institute of Thermal Engineering, Beijing Jiaotong University, Beijing 100044, People's Republic of China

X.-D. Wang
State Key Laboratory of Alternate Electrical Power System with Renewable Energy Sources, North China Electric Power University, Beijing 102206, People's Republic of China

X.-D. Wang
Beijing Key Laboratory of Multiphase Flow and Heat Transfer for Low Grade Energy, North China Electric Power University, Beijing 102206, People's Republic of China

Introduction

Nanofluids as suspensions of nanometer-sized particles are complex fluids widely used in electronic-

cooling, lubrication, and biomedical systems (Choi 1995, 2009; Cheng and Cao 2011; Michaelides 2013). The suspended nanoparticles significantly modify the thermophysical properties of the base fluids so that the nanofluids exhibit attractive properties, such as high thermal conductivity, tunable surface tension, viscosity, and rheology (Chakraborty and Padhy 2008; Trisaksri and Wongwises 2007; Branson et al. 2013). These properties strongly affect the heat transfer, flow, and dynamic wetting behavior of nanofluids in microfluidic systems (Wu et al. 2013; Murshed et al. 2008a; Li et al. 2009); hence, nanofluids can be used as "smart materials" in many applications.

Most previous studies of the thermophysical properties of nanofluids have explored the effects of the nanofluid parameters, such as the nanoparticle loading, diameter and material and the base fluid type on the thermal conductivity, surface tension, viscosity, and rheology. There are a large number of studies on the thermal conductivity (Choi 1995, 2009; Cheng and Cao 2011; Michaelides 2013; Wu et al. 2013; Murshed et al. 2008b; Li et al. 2009), but only a few studies on the nanofluid surface tension, viscosity, and rheology. As shown in Table 1, the surface tensions of nanofluids have been reported to be increased (Zhu et al. 2010; Moosavi et al. 2010; Tanvir and Li 2012), unchanged (Kumar and Milanova 2009; Chen et al. 2011), or decreased (Das et al. 2003; Vafaei et al. 2009) from that of the base fluids,. Even for the same nanofluid, such as Al$_2$O$_3$/H$_2$O nanofluids, the surface tension was reported to be increased by Zhu et al. (2010), but unchanged by Das et al. (2003). Some studies have tried to qualitatively explain the mechanisms for these changes in the nanofluid surface tension (Tanvir and Li 2012; Murshed et al. 2008c; Radiom et al. 2010; Liu and Kai 2012). Tanvir and Li (2012) suggested that the attractive forces between the particles at the liquid–vapor interface increase as the particle concentration increases which increases the surface tension. However, Murshed et al. (2008a), Radiom et al. (2010), and Liu and Kai (2012) proposed that the surface tension reduction may be attributed to the reduction of the cohesive energy at the liquid–vapor interface, since nano-sized particles, when functioning as surfactant molecules, are brought to the lowest interfacial energy location by the Brownian motion. However, all these analyses were only suggestions without providing any direct evidence and some were even contradictory.

Table 1 Studies of the surface tension of nanofluids

Authors	Nanofluids	Method	γ
Zhu et al. (2010)	Al$_2$O$_3$/H$_2$O	Experiment	Increase
Moosavi et al. (2010)	ZnO/EG/glycerol	Experiment	Increase
Tanvir and Li (2012)	Al/Al$_2$O$_3$/B/ MWCNT·H$_2$O	Experiment	Increase
Kumar and Milanova (2009)	CNT/H$_2$O	Experiment	Increase
Chen et al. (2011)	laponite/Fe$_2$O$_3$/ Ag/H$_2$O	Experiment	Constant/ decrease
Das et al. (2003)	Al$_2$O$_3$/H$_2$O	Experiment	Constant
Vafaei et al. (2009)	Bi$_2$Te$_3$/AOT	Experiment/ model	Decrease/ increase
Murshed et al. (2008a)	TiO$_2$/H$_2$O	Experiment	Decrease
Radiom et al. (2010)	TiO$_2$/H$_2$O	Experiment	Decrease
Liu and Kai (2012)	TiN/SiC/Al$_2$O$_3$/ CNT/ammonia– H$_2$O	Experiment	TiN/SiC decrease Al$_2$O$_3$/CN increase

Micro/milli size particles in suspension (colloidal suspensions) increase the base fluid viscosity with several classical models proposed to predict the effective viscosity of colloid suspensions (Einstein 1956; Krieger and Dougherty 1959; Nielsen 1970; Batchelor 1977). However, the viscosity increase for nanofluids is quite different from that of colloidal suspensions with the effective viscosity of nanofluids being quite different from that given by the classical models (Chandrasekar et al. 2010; Nguyen et al. 2008; Lee et al. 2008). The studies of nanofluid viscosity have been reviewed by Eastman et al. (2004), Keblinski et al. (2005), and Mahbubul et al. (2012). Most of these models were only based on hypotheses or empirical correlations between the effective viscosity and macroscopic parameters, such as the loading concentration and temperature. Some correlations considered the effects of particle size as it relates to the Brownian motion (Masoumi et al. 2009; Hosseini et al. 2010); however, undetermined constants in these models must be fit from macroscopic experimental measurements. Thus, more studies are needed to identify the enhancement mechanism with microscopic evidence.

Table 2 Studies of the rheology of nanofluids

Authors	Nanofluids	Method	Rheology
Das et al. (2003)	Al_2O_3/H_2O CuO/H_2O	Experiment	Newtonian
Prasher et al. (2006)	Al_2O_3/PG	Experiment	Newtonian
Chen et al. (2007a)	TiO_2/ethylene glycol	Experiment	Newtonian
Susan-Resiga et al. (2012)	Fe_3O_4/MOL	Experiment	Newtonian
Wang et al. (1999)	CuO/H_2O/ethylene glycol/Al_2O_3/ H_2O/ethylene glycol/engine oil	Experiment	Non-Newtonian
He et al. (2007)	TiO_2/H_2O	Experiment	Non-Newtonian
Murshed et al. (2008b)	Al_2O_3/H_2O	Experiment	Non-Newtonian
Chen et al. (2009)	TNT/EG	Experiment	Non-Newtonian (shear thinning)
Ding et al. (2006)	CNT/H_2O	Experiment	Non-Newtonian (shear thinning)
Kole and Dey (2011)	Al_2O_3/car coolant CuO/gear oil	Experiment	Non-Newtonian
Yu et al. (2001)	AlN/Eg, AlN/PG	Experiment	$\varphi < 5$ %: Newtonian
			$\varphi > 5$ %: non-Newtonian
Yu et al. (2009)	ZnO/EG	Experiment	$\varphi < 2$ %: Newtonian
			$\varphi > 3$ %: non-Newtonian
Kim et al. (2011)	Al_2O_3/H_2O	Experiment	$\varphi < 2$ %: Newtonian
			3 % $< \varphi < 5$ %: non-Newtonian
Abareshi et al. (2011)	α-Fe_2O_3–glycerol	Experiment	Non-Newtonian@low temperature

The rheological properties of nanofluids were reviewed by Chen et al. (2007b). According to the summary in Table 2, there is still debate about whether nanofluids exhibit Newtonian (Das et al. 2003; Prasher et al. 2006; Chen et al. 2007a; Susan-Resiga et al. 2012) or non-Newtonian (Wang et al. 1999; He et al. 2007; Murshed et al. 2008b; Chen et al. 2009; Ding et al. 2006; Kole and Dey 2011; Yu et al. 2001, 2009; Kim et al. 2011; Abareshi et al. 2011) behavior in experiments. Even for the same nanofluid, such as Al_2O_3/H_2O nanofluids, Newtonian rheological behavior was reported by Das et al. (2003) and Prasher et al. (2006), while non-Newtonian rheological behavior was reported by Wang et al. (1999), Murshed et al. (2008c), Kole and Dey (2011), and Kim et al. (2011). Most of these studies only reported experimental data, with few focusing on the mechanisms for the rheological transformation from Newtonian to non-Newtonian fluids by adding nanoparticles. Yu et al. (2009) stated that Newtonian or non-Newtonian behavior of nanofluids depends strongly on many factors, such as the kind and shape of the nanoparticles, the volume fractions, and temperatures. Chen et al. (2007b) proposed an aggregation mechanism to interpret the rheological behavior of nanofluids and categorized the rheological behavior of nanofluids into four groups as dilute, semi-dilute, semi-concentrated,

and concentrated. However, no direct evidence was provided to support their assumptions.

Most previous studies of nanofluids have focused on properties data measurements. The macroscopic measurements were then used to build models to explain the mechanisms; however, these explanations have not been supported by direct evidence. MD simulations can show the microscopic mechanisms for the molecular interactions in much greater detail to provide a microscopic understanding of the thermo-physical properties. MD simulations have been extensively used to investigate the surface tension, viscosity, and rheology of pure liquids (Shi et al. 2006; Mountain 2009; Zhu and Yang 2011; Rutkevych et al. 2010; Hou et al. 2009; Sunda and Venkatnathan 2013; Medina et al. 2011; Thomas and Rowley 2011) or binary mixture solutions (Li et al. 2011; D'Auria and Tobias 2009; Ge et al. 2011; Chen et al. 2010; Kumar et al. 2013). Recently, the MD approach has also been used to model the thermal conductivity of nanofluids (Mohebbi 2012; Cui et al. 2011; Li et al. 2008, 2010; Teng et al. 2008; Sarkara and Selvam 2007) with some results verifying the theories based on macroscopic measurements. However, no MD studies exist that simulate the surface tension, viscosity, and rheology of nanofluids.
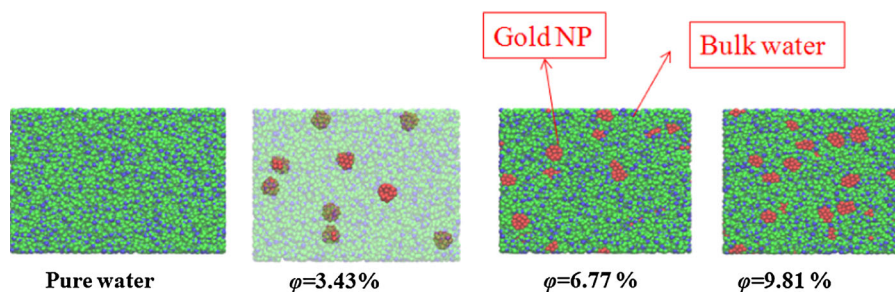
The objective of this work is to study how nanoparticles alter the surface tension, viscosity, and rheology of nanofluids from microscopic viewpoints using MD simulations. The simulations used gold–water nanofluids with the interaction potential parameters varied to represent various types of nanofluids. The microscopic pictures of the nanoparticle–water molecule interactions are used to identify the microscopic mechanisms that explain the modified nanofluid surface tension, viscosity, and rheology.

Simulation methods

Simulation systems

The simulated systems had four nanofluid loadings as shown in Fig. 1. Bulk water films (4,500 water molecules) were simulated at 300 K using molecular dynamics (MD) simulations with four gold nanoparticle loadings (particle volume fractions $\varphi = 0$, 3.43, 6.77, and 9.81 %). The gold nanoparticles ($0.8 \times 0.8 \times 0.8$ nm³ with 32 gold atoms per particle) were equilibrated at 300 K and then absorbed spontaneously by the water film until the nanofluid system reached its minimum energy where the nanoparticles were randomly distributed inside the liquid films, as shown in Fig. 1. The water–water interactions were calculated using the TIP4P-Ew water model (Horn et al. 2004) with the long-range Coulombic forces calculated using the particle–particle particle-mesh technique with the water molecules kept rigid by the SHAKE algorithm (Ryckaert et al. 1977). The gold–gold interactions were calculated using the embedded-atom method (Daw et al. 1993). The 12-6 LJ potential was used to describe the water–gold interactions. The gold nanoparticle wettability was modified by changing the gold–water interaction parameter ε ($\varepsilon = 0.0070$, 0.02714, 0.05427, and 0.08141 eV, with $\sigma = 3.1$ Å and a cutoff distance

of 9 Å). The simulations were performed using LAMMPS (Plimpton 1995) with NVT ensembles at $T = 300$ K with a time step of 1 fs in all cases.

Surface tension calculation method

In most MD simulations, the surface tension is calculated based on the Young–Laplace equation (Ismail et al. 2006).

$$\Delta p = \frac{\gamma_{lv}}{R}, \tag{1}$$

where Δp is the pressure difference between the inside and outside of the droplet, γ_{lv} is the liquid–vapor surface tension, and R is the droplet radius. However, the pressure fluctuates greatly in LAMMPS. For example, for a set pressure of 1 bar, the standard deviation of the fluctuations is about 40 bar. Thus, the surface tension cannot be calculated with such large pressure variations even with time averaging. Therefore, the new method was used to calculate the surface tension of the liquid vapor system. Another NVT system was simulated with a nanofluid film with two free surfaces. The time-averaged excess energy of the two systems with and without free surfaces was then used to calculate the surface tension for pure water and for the nanofluids with different particle loadings as

$$\gamma_{lv} = \frac{\langle E_{\mathrm{w}} \rangle - \langle E_{\mathrm{w/o}} \rangle}{A_{\mathrm{interface}}}, \tag{2}$$

where $\langle E \rangle$ is the time-averaged total energy, the subscripts w and w/o denote with and without liquid–vapor interfaces, and $A_{\mathrm{interface}}$ is the area of the free interface.

Viscosity and rheology calculation method

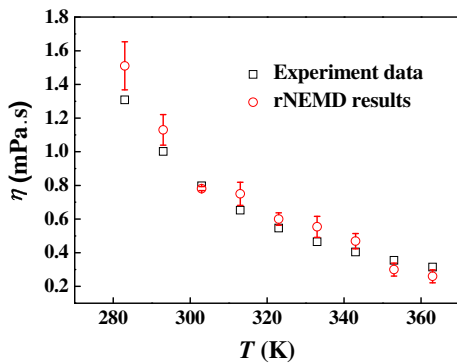The reverse non-equilibrium MD (rNEMD) method (Muller-Plathe 1999) was used to calculate the

Fig. 2 Verification of the rNEMD method: viscosity of pure water at various temperatures

nanofluid viscosity since it is more robust than the equilibrium MD method. The method is based on Onsager linear response theory,

$$j_\alpha = -\sum_\beta L_{\alpha\beta} X_\beta, \qquad (3)$$

where j_α is the momentum flux, X_β is the driving force (velocity gradient), and $L_{\alpha\beta}$ is the diffusion coefficient (viscosity).

A momentum flux was imposed on the bulk liquid to generate a velocity gradient. The diffusion coefficient, in this case the viscosity, was then obtained using

$$j_\alpha \langle p_x \rangle = \frac{P_x}{2tA}, \qquad (4)$$

where P_x is the pressure in the x direction, t the velocity swapping period, and A is xy plane area.

To impose the momentum flux onto the bulk liquid, two water molecules were moved in the bottom and middle plates against the intended current, one with the minimum velocity and the other with the maximum velocity. The velocities were then swapped in another calculation. The momentum flux then generated a velocity gradient, dV_x/dz. A good linear velocity profile was obtained along the z direction that was fit with a straight line with the momentum flux then calculated using Eq. (4).

The velocity swapping period, t, in Eq. (4) was varied to create various momentum fluxes and velocities to relate the viscosity to the shear rate (rheology).

The MD results agree well with experimental data for pure water at various temperatures as shown in Fig. 2 which indicates the accuracy of the present water model and the rNEMD method.

Results and discussion

Surface tension of gold–water nanofluids

For pure water, the calculated surface tension from the MD simulations was $\gamma = 0.0679$ N/m at $T = 300$ K which differs by 5.6 % from the experimental value of $\gamma = 0.072$ N/m (Gittens 1969). The addition of nanoparticles increased the surface tension of the nanofluid with $\varphi = 3.43$ % for $\varepsilon_{water-gold} = 0.05427$ eV, but reduced it for $\varepsilon_{water-gold} = 0.0070$ eV. The different tendencies for these two cases are related to the different water–gold interactions ($\varepsilon_{water-gold}$) and water–water interactions ($\varepsilon_{water-water} = 0.0071$ eV for TIP4P-Ew). For $\varepsilon_{water-gold} < \varepsilon_{water-water}$, the nanoparticles are hydrophobic, so they tend to stay on the free surface, acting as surfactant-like particles, as shown in Fig. 3a. For $\varepsilon_{water-gold} > \varepsilon_{water-water}$, the nanoparticles are hydrophilic, so they tend to submerge into the bulk liquid, acting as non-surfactant particles, as shown in Fig. 3b.

The surface tension indicates the unbalanced forces acting on the liquid molecules on the interface due to the van der Waals force, as shown in Fig. 4a. The liquid molecules at the surface do not have an equal number of molecules on the vapor side so they are pulled inwards by the internal molecules which results in the surface tension which forces the liquid surface to contract to the minimum area. Thus, the nanoparticle wettability is responsible for the different surface tensions. For hydrophobic nanoparticles, the nanoparticles gather on the free surface. The repulsion force between the nanoparticles and the water molecules increases the intermolecular spacing at the interface and reduces the attraction forces between the water molecules inside the bulk liquid and the ones on the free surface regions; thus reducing the surface tension, as shown in Fig. 4b. However, some hydrophilic nanoparticles are transported toward the interfacial region by Brownian motion where the attraction forces between the nanoparticles and the water molecules reduce the intermolecular spacing at the interface. The water molecules at the free surface are more strongly pulled inwards due to the presence of the hydrophilic nanoparticles with stronger gold–water interaction forces than for the water–water interactions, which increase the surface tension, as shown in Fig. 4c.

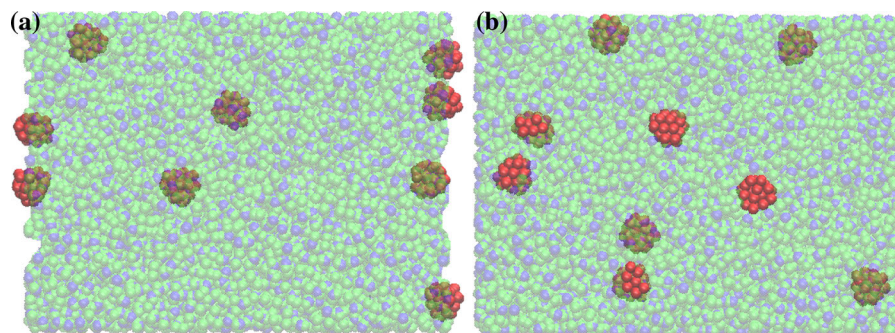Figure 5 shows the evidence for the hydrophobic/hydrophilic nanoparticles changing the intermolecular

Fig. 3 Snapshots of the 3.43 % nanofluid with **a** hydrophobic gold nanoparticles ($\varepsilon = 0.007$ eV); **b** hydrophilic gold nanoparticles ($\varepsilon = 0.05427$ eV)
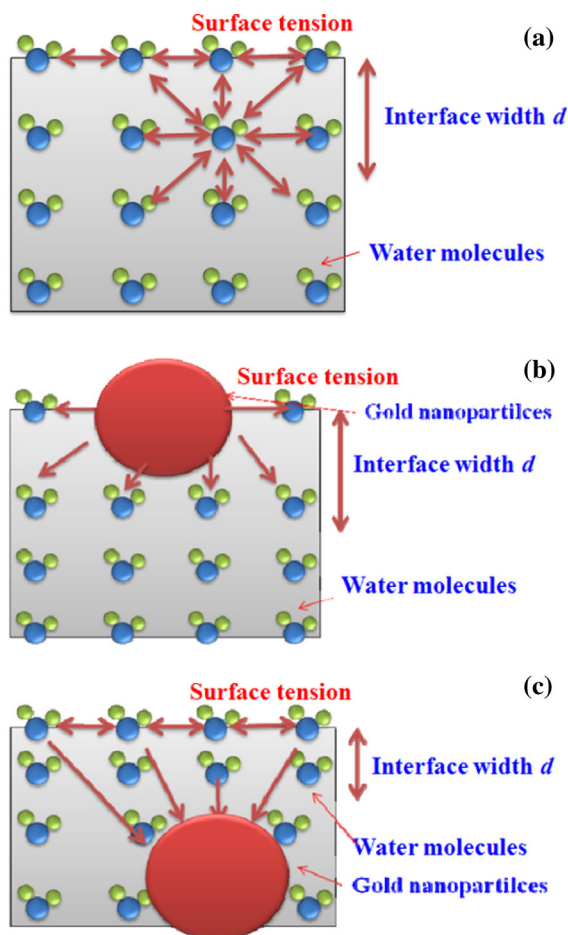

Fig. 4 Schematic of the van der Waals force between water molecules and nanoparticle–water molecule near the interface region: **a** water molecular interaction for pure water; **b** gold nanoparticle–water molecule interactions for $\varepsilon_{water–gold} < \varepsilon_{water–water}$; **c** gold nanoparticle–water molecule interactions for $\varepsilon_{water–gold} < \varepsilon_{water–water}$
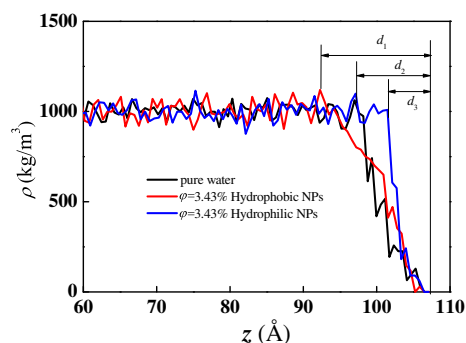

Fig. 5 Water density profiles perpendicular to the free surface for pure water and nanofluids with hydrophobic or hydrophilic nanoparticles ($\varphi = 3.43$ %)

spacing in the interface region. The water density remains constant in the bulk liquid but decreases sharply near the interface. The thickness of the reduced density region, defined as the interface width, d, decreases with increasing nanoparticle wettability, leading to the increased surface tension. In addition, the interface width, d, decreases with increasing φ for the hydrophilic nanoparticles, but increases with increasing φ for the hydrophobic nanoparticles.

Viscosity of gold–water nanofluids

The viscosities of pure water and low loading nanofluids ($\varphi = 0$ %, $\varphi = 3.43$ % and $\varphi = 6.77$ %) are shown in Fig. 6. The viscosity increases with increasing volume concentration, which is consistent with experimental data (Hilsenrath 1995). The increasing viscosity with loading is illustrated by the microscopic
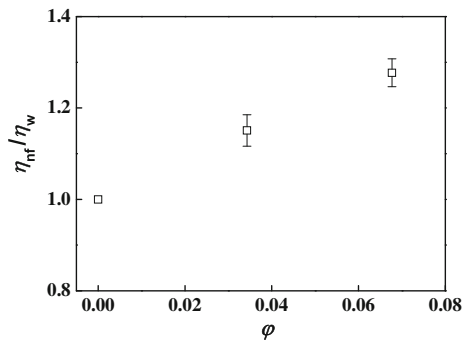
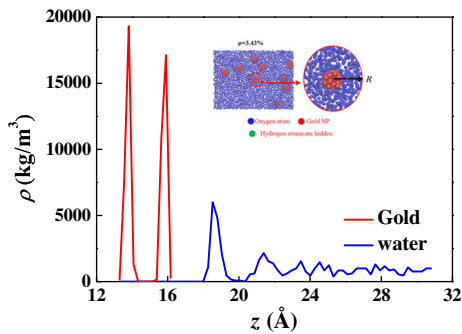**Fig. 6** Nanofluid viscosity for various NP loadings

Fig. 7 Water density near a gold nanoparticle (*inset* illustration of the water molecule layer)

picture of one randomly selected gold nanoparticle shown in the insert in Fig. 7, in which the hydrogen atoms are hidden. An absorbed water layer has formed around the gold nanoparticle which can be seen by the water density plotted along the radial direction in Fig. 7. The water density near the nanoparticle at 19 Å is five times that of the bulk liquid, indicating a solid-like absorbed water layer around the gold nanoparticle. The effect can be explained by the Einstein diffusion equation (Einstein 1905),

$$D_{NP} = \frac{k_B T}{6\pi\eta r}, \tag{5}$$

where D_{NP} is the nanoparticle diffusion coefficient, k_B is Boltzmann's constant, T is the absolute temperature, η is the base liquid viscosity, and r is the particle radius. The absorbed water layer increases the equivalent nanoparticle radius which hinders nanoparticle diffusion within the base liquid according to Eq. (5). Consequently, the increased nanofluid viscosity can be explained by the decreased nanoparticle diffusion coefficient. The absorbed layer is also the basis for the
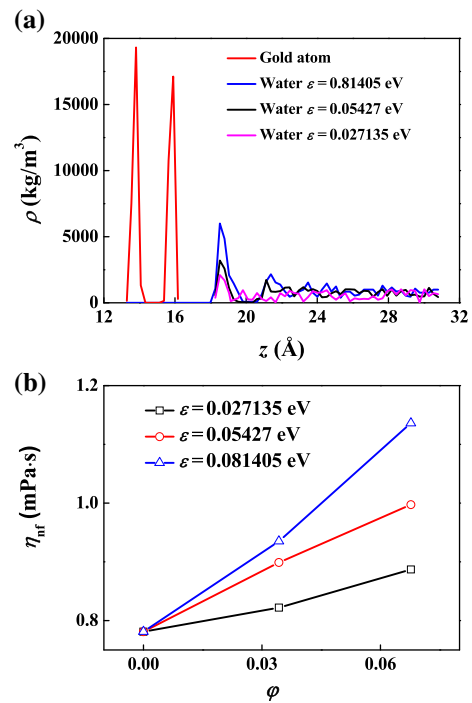

Fig. 8 Effects of gold nanoparticle–water molecule interactions on **a** atom number density; **b** viscosity

nanofluid thermal conductivity enhancement mechanism (Li et al. 2008, 2010). The interactions between the nanoparticles and the water molecules were changed by modifying ε. As shown in Fig. 8a, the density of the absorbed water layer increases with the increasing gold–water interaction parameter. Thus, smaller diffusion coefficients occur for stronger NP-water molecule interactions and the nanofluid viscosity can be expected to increase with increasing of the gold–water interaction parameter, as can be seen in Fig. 8b. The number of gold nanoparticles in the solution affects the viscosity, as shown in Fig. 8b, but does not affect the intensity of the absorbed water layer for a single nanoparticle if the nanoparticle loading is low enough.

Rheology of gold–water nanofluids

The viscosity versus shear rate variation is shown in Fig. 9. For pure water and low nanofluid loadings ($\varphi = 3.43$ %) and $\varphi = 6.77$ %), the viscosity remains constant for shear rates from 10^{-1} to 3×10^2 s^{-1}. However, the viscosity of the $\varphi = 9.81$ % nanofluid remains constant only with a narrow shear rate range
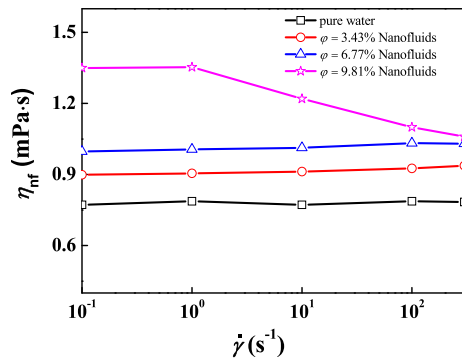
Fig. 9 Viscosity versus shear rate (rheology) for nanofluids for various loadings ($\varepsilon = 0.05427$ eV)

Fig. 10 Solidification effect at high loadings (*inset* illustration of the molecular spacing)

Fig. 11 Effects of gold nanoparticle–water molecule interactions on the rheology for $\varphi = 3.43$ % and $\varphi = 6.77$ % nanoparticle loadings

(from 10^{-1} to 10^{0} s^{-1}) and decreases as the shear rate increases from 10^{0} to 3×10^{2} s^{-1}, indicating shear-thinning non-Newtonian rheological behavior. This rheology transformation at high shear rates was also seen experimentally by Carré and Woehl (2006).

The nanoparticles move randomly in the base liquid due to Brownian motion. Comparison of the particle distribution with the high loading in the insert in Fig. 10 with the distribution for a lower loading seen in the insert in Fig. 7 shows that there are more chances for nanoparticles to move closer together for high loadings. A typical microscopic structure of two nanoparticle–water molecule cluster is shown in the insert in Fig. 10. The solid-like absorbed water layers around the nanoparticles are also observed in this structure. Additionally, the water density between these two closed nanoparticles is several times larger than that of the bulk liquid density, as shown in Fig. 10, indicating that solidification of the water molecules also occurs in this structure, which defined here as a solidification structure due to the additional nanoparticle–nanoparticle interactions. This solidification structure further increases the nanofluid viscosity for higher loadings. The solidification structures remain unchanged at low shear rates, where the nanofluids exhibit Newtonian rheological behavior. However, there is a critical shear rate above which the solidification structures are disrupted and the solidified water molecules move more freely, which reduces the nanofluid viscosity, leading to the shear-thinning rheological behavior.

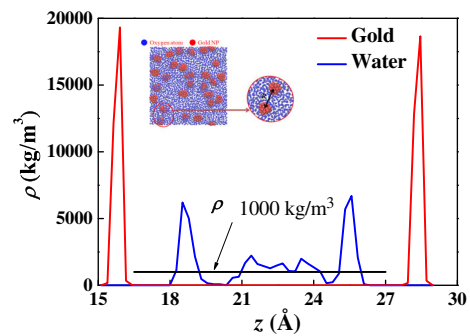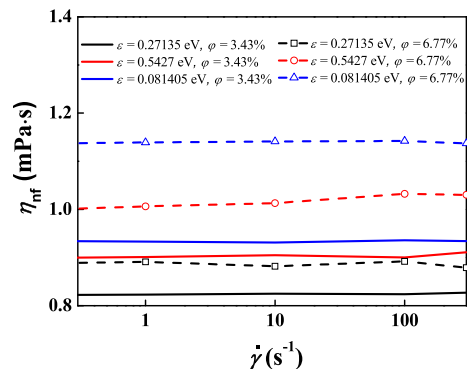When the gold–water interactions increase for lower loadings ($\varphi = 3.43$ % and $\varphi = 6.77$ %), the viscosity increases while the rheology remains unchanged, as shown in Fig. 11. Therefore, the mechanism for the solidification effect, which is more likely at high loadings is related to but differs from the mechanism for the solid-like absorbed water layer that alters the viscosity.

Conclusions

The surface tension, viscosity, and rheology of gold–water nanofluids were examined using MD simulations. The effects of the gold nanoparticle loadings and particle wettability were examined. The main conclusions are

(1)   The microscopic mechanism for the surface tension variation is related to the nanoparticle wettability. The repulsion of water molecules by surfactant-like nanoparticles increases the molecular spacing on the free surface which

reduces the fluid surface tension. The attraction induced by non-surfactant nanoparticles reduces the molecular spacing on the free surface which increases the surface tension.

(2) A solid-like absorbed water layer around the nanoparticles increases the equivalent nanoparticle radius and hinders the nanoparticle mobility within the base fluid which increases the nanofluid viscosity.

(3) The nanofluid rheological behavior depends on the nanoparticle loading. For low loadings, the viscosity increases with increasing gold–water interaction forces, but remains unchanged with the shear rate, indicating Newtonian behavior. For high loadings, water molecule solidification is observed between neighboring nanoparticles due to the strong nanoparticle–nanoparticle interactions. These solidification structures are then disrupted for shear rates exceeding a critical value, which leads to shear-thinning non-Newtonian behavior.

References

Abareshi M, Sajjadi SH, Zebarjad SM, Goharshadi EK (2011) Fabrication, characterization, and measurement of viscosity of α-Fe_2O_3–glycerol nanofluids. J Mol Liquids 163(1):27–32

Batchelor GK (1977) The effect of Brownian motion on the bulk stress in a suspension of spherical particles. J Fluid Mech 83(1):97–117

Branson BT, Beauchamp PS, Beam JC, Lukehart CM, Davidson JL (2013) Nanodiamond nanofluids for enhanced thermal conductivity. ACS Nano 7(4):3183–3189

Carré A, Woehl P (2006) Spreading of silicone oils on glass in two geometries. Langmuir 22(1):134–139

Chakraborty S, Padhy S (2008) Anomalous electrical conductivity of nanoscale colloidal suspensions. ACS Nano 2(10):2029–2036

Chandrasekar M, Suresh S, Chandra BA (2010) Experimental investigations and theoretical determination of thermal conductivity and viscosity of Al_2O_3/water nanofluids. Exp Therm Fluid Sci 34(2):210–216

Chen HS, Ding YL, He YR, Tan CQ (2007a) Rheological behaviour of ethylene glycol based titania nanofluids. Chem Phys Lett 444(4–6):333–337

Chen HS, Ding YL, Tan CQ (2007b) Rheological behaviour of nanofluids. New J Phys 9:367

Chen HS, Ding YL, Lapkin A (2009) Rheological behaviour of nanofluids containing tube rod-like nanoparticles. Powder Technol 194(1–2):132–141

Chen T, Chidambaram M, Liu ZP, Smit B, Bell AT (2010) Viscosities of the mixtures of 1-ethyl-3-methylimidazolium chloride with water, acetonitrile and glucose: a molecular dynamics simulation and experimental study. J Phys Chem B 114(17):5790–5794

Chen RH, Phuoc TX, Martello D (2011) Surface tension of evaporating nanofluid droplets. Int J Heat Mass Transf 54:2459–2466

Cheng LS, Cao DP (2011) Designing a thermo-switchable channel for nanofluidic controllable transportation. ACS Nano 5(2):1102–1108

Choi SUS (1995) Enhancing thermal conductivity of fluids with nanoparticles. In: Siginer DA, Wang HP (eds) Developments and application of non-Newtonian flows, FED 231/MD, vol 66. ASME, New York, pp 99–105

Choi SUS (2009) Nanofluids: from vision to reality through research. J Heat Transf 131(3): 033106-1–033106-9

Cui WZ, Bai ML, Lv JZ (2011) On the influencing factors and strengthening mechanism for thermal conductivity of nanofluids by molecular dynamics simulation. Ind Eng Chem Res 50(23):13568–13575

D'Auria R, Tobias DJ (2009) On the relation between surface tension and ion adsorption at the air–water interface: a molecular dynamics simulation study. J Phys Chem A 113(26):7286–7293

Das SK, Putra N, Reotzel W (2003) Pool boiling characteristics of nano-fluids. Int J Heat Mass Transf 46:851–862

Daw DS, Foiles SM, Baskes MI (1993) The embedded atom method: a review of theory and applications. Mater Sci Rep 9(7–8):251–310

Ding Y, Alias H, Wen D, Williams AR (2006) Heat transfer of aqueous suspensions of carbon nanotubes (CNT nanofluids). Int J Heat Mass Transf 49(1):240–250

Eastman JA, Phillpot SR, Choi SUS, Keblinski P (2004) Thermal transport in nanofluids. Annu Rev Mater Res 34:219–246

Einstein A (1905) Über die von der molekularkinetischen Theorie der Wärme geforderte Bewegung von in ruhenden Flüssigkeiten suspendierten Teilchen. Ann Phys 322:549–560

Einstein A (1956) Investigations on the theory of Brownian movement. Dover, New York

Ge S, Zhang XX, Chen M (2011) Viscosity of NaCl aqueous solution under supercritical conditions: a molecular dynamics simulation. J Chem Eng Data 56(4):1299–1304

Gittens GJ (1969) Variation of surface tension of water with temperature. J Colloid Interface Sci 30(3):406–412

He Y, Jin Y, Chen HS, Ding Y, Cang D, Lu H (2007) Heat transfer and flow behaviour of aqueous suspensions of TiO_2 nanoparticles (nanofluids) flowing upward through a vertical pipe. Int J Heat Mass Transf 50(11–12):2272–2281

Hilsenrath J (1995) US National Bureau of Standards Circuits No. 564

Horn HW, Swope WC, Pitera JW, Madura JD, Dick TJ, Hura GL, Head-Gordon T (2004) Development of an improved

four-site water model for biomolecular simulations: tIP4P-Ew. J Chem Phys 120(20):9665–9677

Hosseini SM, Moghadassi AR, Henneke DE (2010) A new dimensionless group model for determining the viscosity of nanofluids. J Therm Anal Calorim 100:873–877

Hou HY, Chen GL, Chen G (2009) A molecular dynamics simulation on surface tension of liquid Ni and Cu. Comput Mater Sci 46(1):516–519

Ismail AE, Grest GS, Stevens MJ (2006) Capillary waves at the liquid–vapor interface and surface tension of water models. J Chem Phys 125(1):014702

Keblinski P, Eastman JA, Cahill DG (2005) Nanofluids for thermal transport. Mater Today 8(6):36–44

Kim S, Kim C, Lee WH, Park SR (2011) Rheological properties of alumina nanofluids and their implication to the heat transfer enhancement mechanism. J Appl Phys 110(3):34316

Kole M, Dey TK (2011) Effect of aggregation on the viscosity of copper oxide–gear oil nanofluids. Int J Therm Sci 50(9):1741–1747

Krieger IM, Dougherty TJ (1959) A mechanism for non-New-tonian flow in suspension of rigid spheres. Trans Soc Rheol 3:137–152

Kumar R, Milanova D (2009) Effect of surface tension on nanotube nanofluids. Appl Phys Lett 94:073107

Kumar P, Varanasi SR, Yashonath S (2013) Relation between the diffusivity, viscosity, and ionic radius of LiCl in water, methanol, and ethylene glycol: a molecular dynamics simulation. J Phys Chem B 117(27):8196–8208

Lee JH, Hwang KS, Janga S, Lee BH, Kim JH, Choi SUS, Choi CJ (2008) Effective viscosities and thermal conductivities of aqueous nanofluids containing low volume concentrations of Al_2O_3 nanoparticles. Int J Heat Mass Transf 51(11–12):2651–2656

Li L, Zhang YW, Ma HB, Yang M (2008) An investigation of molecular layering at the liquid-solid interface in nanofluids by molecular dynamics simulation. Phys Lett A 372(25):4541–4544

Li YJ, Zhou JE, Tung S, Schneider E, Xi SQ (2009) A review on development of nanofluid preparation and characterization. Powder Technol 196:89–101

Li L, Zhang YW, Ma HB, Yang M (2010) Molecular dynamics simulation of effect of liquid layering around the nano-particle on the enhanced thermal conductivity of nanofluids. J Nanopart Res 12(3):811–821

Li X, Hede T, Tu Y (2011) Glycine in aerosol water droplets: a critical assessment of Köhler theory by predicting surface tension from molecular dynamics simulations. Atmos Chem Phys 11:519–527

Liu Y, Kai D (2012) Investigations of surface tension of binary nanofluids. Adv Mater Res 347–353:786–790

Mahbubul IM, Saidur R, Amalina MA (2012) Latest develop-ments on the viscosity of nanofluids. Int J Heat Mass Transf 55(4):874–885

Masoumi N, Sohrabi N, Behzadmehr A (2009) A new model for calculating the effective viscosity of nanofluids. J Phys D Appl Phys 42:055501

Medina JS, Prosmiti R, Villarreal P (2011) Molecular dynamics simulations of rigid and flexible water models: temperature dependence of viscosities. Chem Phys 388(1–3):9–18

Michaelides EE (2013) Transport properties of nanofluids. A critical review. J Non-Equilib Thermodyn 38(1):1–79

Mohebbi A (2012) Prediction of specific heat and thermal conductivity of nanofluids by a combined equilibrium and non-equilibrium molecular dynamics simulation. J Mol Liquids 175:51–58

Moosavi M, Goharshadi EK, Youssefi A (2010) Fabrication, characterization, and measurement of some physico-chemical properties of ZnO nanofluids. Int J Heat Mass Transf 31(4):599–605

Mountain RD (2009) An internally consistent method for the molecular dynamics simulation of the surface tension: application to some tip4p-type models of water. J Phys Chem B 113(2):482–486

Muller-Plathe F (1999) Reversing the perturbation in nonequi-librium molecular dynamics: an easy way to calculate the shear viscosity of fluids. Phys Rev E 59(5):4894–4898

Murshed SMS, Leoong KC, Yang C (2008a) Thermophysical and electrokinetic properties of nanofluids—a critical review. Appl Therm Eng 28(17–18):2109–2125

Murshed SMS, Leong KC, Yang C (2008b) Investigations of thermal conductivity and viscosity of nanofluids. Int J Therm Sci 47(5):560–568

Murshed SMS, Tan SH, Nguyen NT (2008c) Temperature dependence of interfacial properties and viscosity of nanofluids for droplet-based microfluidics. J Phys D Appl Phys 41(8):085502

Nguyen CT, Desgranges F, Galanis N, Roy G, Maré T, Boucher S, Mintsa HA (2008) Viscosity data for Al_2O_3–water nanofluid-hysteresis: is heat transfer enhancement using nanofluids reliable. Int J Therm Sci 47(2):103–111

Nielsen LE (1970) Generalized equation for the elastic moduli of composite materials. J Appl Phys 41(11):4626–4627

Plimpton S (1995) Fast parallel algorithms for short-range molecular dynamics. J Comput Phys 117(1):1–19

Prasher R, Song D, Wang J, Phelan PE (2006) Measurements of nanofluid viscosity and its implications for thermal appli-cations. Appl Phys Lett 89:133108-1–133108-3

Radiom M, Yang C, Chan WK (2010) Characterization of sur-face tension and contact angle of nanofluids. Proc SPIE 7522:75221D

Rutkevych PP, Ramanarayan H, Wu DT (2010) Optimizing the computational efficiency of surface tension estimates in molecular dynamics simulations. Comput Mater Sci 49(1):s95–s98

Ryckaert JP, Ciccotti G, Berendsen HJC (1977) Numerical integration of the cartesian equations of motion of a system with constraints: molecular dynamics of n-alkanes. J Comput Phys 23(3):327–341

Sarkara S, Selvam SP (2007) Molecular dynamics simulation of effective thermal conductivity and study of enhanced thermal transport mechanism in nanofluids. J Appl Phys 102(2):074302

Shi B, Sinha S, Dhir VK (2006) Molecular dynamics simulation of the density and surface tension of water by particle–particle particle–mesh method. J Chem Phys 124(20):204715

Sunda AP, Venkatnathan A (2013) Parametric dependence on shear viscosity of SPC/E water from equilibrium and non-equilibrium molecular dynamics simulations. Mol Simul 39(9):728–733

Susan-Resiga D, Socoliuc V, Boros T, Borbath T, Marinica O, Han A, Vekas L (2012) The influence of particle clustering on the rheological properties of highly concentrated magnetic nanofluids. J Colloid Interface Sci 373(1):110–115

Tanvir S, Li Q (2012) Surface tension of nanofluid-type fuels containing suspended nanomaterials. Nanoscale Res Lett 7:226–236

Teng KL, Hsiao PY, Hung SW, Chieng CC, Liu MS, Lu MC (2008) Enhanced thermal conductivity of nanofluids diagnosis by molecular dynamics simulations. J Nanosci Nanotechnol 8(7):3710–3718

Thomas JC, Rowley RL (2011) Transient molecular dynamics simulations of liquid viscosity for nonpolar and polar fluids. J Chem Phys 134(2):024526

Trisaksri V, Wongwises S (2007) Critical review of heat transfer characteristics of nanofluids. Renew Sustain Energy Rev 11(3):512–523

Vafaei S, Purkayastha A, Jain A (2009) The effect of nanoparticles on the liquid-gas surface tension of Bi_2Te_3 nanofluids. Nanotechnology 20(18):185702

Wang XW, Xu XF, Choi SUS (1999) Thermal conductivity of nanoparticle–fluid mixture. J Therm Heat Transf 13(4):474–480

Wu S, Nikolov A, Wasan D (2013) Cleansing dynamics of oily soil using nanofluids. J Colloid Interface Sci 396:293–306

Yu W, Xie H, Li Y, Chen L (2001) Experimental investigation on thermal conductivity and viscosity of aluminum nitride nanofluid. Particuology 9(2):187–191

Yu W, Xie H, Chen L, Li Y (2009) Investigation of thermal conductivity and viscosity of ethylene glycol based ZnO nanofluids. Thermochim Acta 491(1–2):92–96

Zhu RZ, Yang H (2011) A new method for the determination of surface tension from molecular dynamics simulations applied to liquid droplets. Chin Phys B 20(1):016801

Zhu D, Wu S, Wang N (2010) Thermal physics and critical heat flux characteristics of Al_2O_3-H_2O nanofluids. Heat Transf Eng 31:1213–1219